FINITE ELEMENT ANALYSIS OF DISC TEMPERATURE DURING BRAKING PROCESS

Piotr GRZEŚ*

*Faculty of Mechanical Engineering, Białystok Technical University, ul. Wiejska 45 C, 15-351 Białystok

p.grzes@doktoranci.pb.edu.pl

Abstract: The aim of this paper was to investigate the temperature fields of the solid disc brake during short, emergency braking. The standard Galerkin weighted residual algorithm was used to discretize the parabolic heat transfer equation. The finite element simulation for two-dimensional model was performed due to the heat flux ratio constantly distributed in circumferential direction. Two types of disc brake assembly with appropriate boundary and initial conditions were developed. Results of calculations for the temperature expansion in axial and radial directions are presented. The effect of the angular velocity and the contact pressure evolution on temperature rise of disc brake was investigated. It was found that presented finite element technique for two-dimensional model with particular assumption in operation and boundary conditions validates with so far achievements in this field.

1. INTRODUCTION

Over decades, frictional heating in brakes and clutches has been investigated by many researches. Temperature rise affected by conversion of large amounts of kinetic energy into heat energy is a complex phenomenon. All characteristics of the process (velocity, pressure, friction coefficient, thermal properties of the materials) vary with time. However, it is important to predict temperature distribution of heat generation during braking and clutch engagement.

Long repetitive braking terms, particularly during mountain descents or high-speed stops (autobahn stop) may cause significant concern. Undesirable effects (low frequency vibrations, fade of the lining with variations of friction coefficient, premature wear, brake fluid vaporization) directly affect braking performance. Hence it is essential to know the peak temperatures at the beginning of the design process.

Talati and Jalalifar (2008, 2009) formulated the problem of two models of heat dissipation in disc brakes: namely macroscopic and microscopic model. In the macroscopic model First Law of Thermodynamics has been taken into account and for microscopic model various characteristics such as duration of braking, material properties, dimensions and geometry of the brake system have been studied. Both disc and pad volume have been investigated to evaluate temperature distributions. The conduction heat transfer was investigated using finite element method (Talati and Jalalifar, 2008). In paper (Talati and Jalalifar, 2009) problem was solved analytically using Green's function approach. Influence of thermomechanical distortions during heat generation has been neglected.

Gao and Lin (2002) investigated non-axisymmetrical model of disc brake system with moving heat source. Appropriate boundary conditions due to analytical model have been imposed. To solve the problem, a transient FE technique has been used. Numerical estimations reveal that the operating parameters of the braking process significantly influence the disc/pad interface temperature distribution and the maximal contact temperature.

According to Ramachandra Rao et al. (1989) it is essential that the analysis is treated as a nonlinear (thermal conductivity and enthalpy for the disc material vary with respect to temperature). In this paper the simulation of the temperature field in the disc brake has been carried out using the finite element method. Both, wear and temperature distribution have been considered. The computer simulation of the fade mechanism using 'clock mechanism' is examined which is also verified with the experimental outcome.

Grieve et al. (1998) compares different materials for pad element of automotive disc brake with its significant weight advantages corresponds to lower maximum operating temperature. Three dimensional model of brake system assembly has been imposed with the finite element method simulation. The author examines the effect of the vehicle mass on the peak disc temperatures. Also Taguchi technique (1993) has been applied to develop influence of all the critical design and material factors.

FE modelling of the heat generation process in a mine winder disc brake is proposed in monograph: Ścieszka and Żołnierz (2007).

In this study, transient thermal analysis of disc brake utilizing finite element method is developed. Both analytical and numerical investigations are performed. Various boundary and operation conditions in two types of FE models with appropriate material properties (Talati and Jalalifar, 2009; Gao and Lin, 2002) are established.

2. REAL PROBLEM

Disc brake consists of cast-iron disc which rotates with the wheel, caliper fixed to the steering knuckle and friction material (brake pads) which is shown in Fig 1. When the braking process occurs, the hydraulic pressure forces the piston and therefore pads and disc brake are in sliding contact. Set up force resists the movement and the vehicle slows down or eventually stops. Friction between disc and pads always opposes motion and the heat is generated due to conversion of the kinetic energy. However, friction surface is exposed to the enlarged air flow for high speed braking and the heat is dissipated.

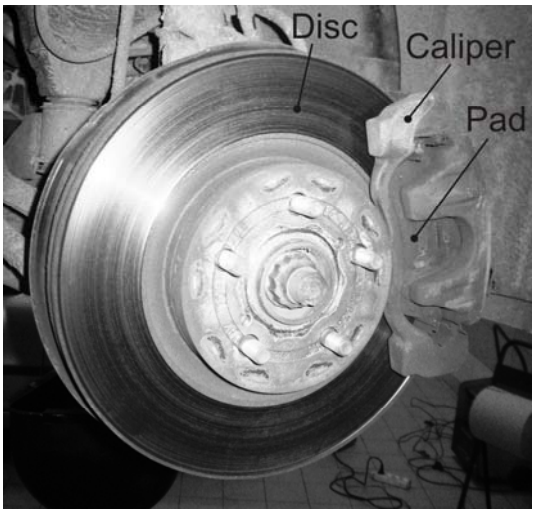

Fig. 1. Front disc brake of the passenger's car

Disc brake. In general disc brakes are made of gray cast iron and are either solid or ventilated. The ventilated types of discs have vanes or fins to increase surface of heat exchange by convection. Furthermore, higher order of disc brakes have drilled holes. Nowadays a cross-drilled discs are commonly used in motorcycles, racing cars or very high performance road cars. Cross-drilled enables more efficient gas release in the brake exert. The disc must have limited mass in order to diminish the inertia forces and non-suspending mass.

Pads. Several assumptions should be considered in the case of design process of friction material. It is known that the value of sliding friction depends of the nature of two surfaces which touch each other. Material selection must deal with the coefficient of friction which is supposed to remain constant in the braking process corresponding to wide variety of disc/pad interface temperature. Also wear is vital in case of braking performance.

Caliper. Generally two types of calipers are commonly used: the floating calipers and the fixed calipers. Depending on the way of operation, the floating caliper has either one or two pistons.

In the floating caliper (Fig. 1) the piston is located only in one side of the disc. Equal pressure at the same time is distributed on the two inner surfaces of pads by using reaction when the pressure acts piston on the one side of the disc.

The fixed caliper have two pistons in both sides of the disc brake. The equilibrium of pressure at any pad is settled by the single source of the hydraulic pressure partitioned to each canal of the piston. This type of caliper is heavier and also larger because of complexity of the disc brake assembly. The advantage is that they absorb more energy by heat dissipation.

3. PHYSICAL PROBLEM

Disc brake system consists of two elements: rotating axisymmetric disc and immovable non-axisymmetric pad (Fig. 2). The most important function of disc brake system in automotive application is to reduce velocity of the vehicle by changing the kinetic energy into thermal energy. When the braking process occurs total heat is dissipated by conduction from disc/pad interface to adjacent components of brake assembly and hub and by convection to atmosphere in accordance to Newton's law. The radiation may be neglected due to relatively low temperature and short time of the braking process.

In this paper for validation of proposed finite element (FE) modeling technique, two types of solid disc brake were analyzed (Fig. 2). Type A according to Talati and Jalalifar's paper (2009) and Type B according to Gao and Lin's paper (2002).

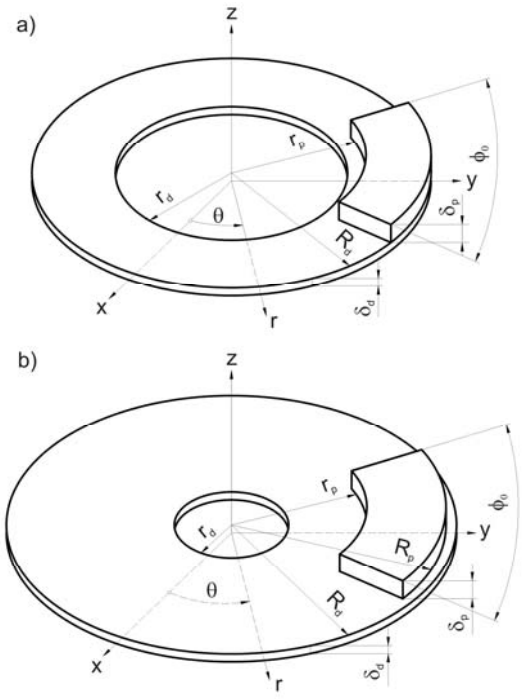

Fig. 2. The schematic representation of disc brake system a) Type A; b) Type B

For both types it has been assumed as follows:

1) Material properties are isotropic and independent of the temperature;
2) The real surface of contact between a disc brake and pad in operation is equal to the apparent surface in the

sliding contact. Hence pressure is uniformly distributed over all friction surfaces;

3) The average intensity of heat flux into disc on the contact area equals (Ling, 1973):

$$q_d(r,z,t)\big|_{z=\delta_d} = \gamma \frac{\phi_0}{2\pi} fp(t) r\omega(t), \quad (1)$$

$$r_p \le r \le R_p, 0 \le t \le t_s,$$

and into pad

$$q_p(r,z,t)\big|_{z=\delta_p} = (1-\gamma) fp(t) r\omega(t), \quad (2)$$

$$r_p \le r \le R_p, 0 \le t \le t_s,$$

where: γ is the heat partitioning factor, ϕ_0 is the cover angle of pad, f is the friction coefficient, p is the contact pressure, ω is the angular velocity, t is the time, t_s is the braking time, r is the radial coordinate, z is the axial coordinate, r_p and R_p are the internal and external radius of the pad. The subscripts p and d imply the pad and the disc respectively;

4) The heat partitioning factor representing the fraction of frictional heat flux entering the disc has the form (Blok, 1940):

$$\gamma = \frac{1}{1+\sqrt{\rho_p c_p K_p / \rho_d c_d K_d}}, \quad (3)$$

where ρ is the density, c is the specific heat and K is the thermal conductivity;

5) The frictional heat due to Newton law has been dissipated to atmosphere on the other surfaces. The heat transfer coefficient h is constant during braking process;

6) Because of short braking time and hence relatively low temperature the radiation is neglected.

Two types of single disc have been analyzed with its simplification to symmetrical problem. Therefore one side of the disc has been insulated in both types of the FE model.

In Type A the single surface of disc symmetry is insulated. Excluding both the surface of symmetry and the surface of sliding contact with the intensity of heat flux boundary condition, on all remaining surfaces the exchange of thermal energy by convection to atmosphere has been implied.

Furthermore in Type B the inner surface of disc was thermally insulated. On the area of sliding contact of disc brake surface intensity of the heat flux has been established. The frictional heat due to Newton law has been dissipated to atmosphere on the other surfaces.

In Type A the contact pressure p is given as follows

$$p = p_0, \quad (4)$$

and the angular velocity ω is linear in time t:

$$\omega(t) = \omega_0\left(1 - \frac{t}{t_s^0}\right), \ 0 \le t \le t_s^0 \quad (5)$$

where: p_0 is the nominal pressure, ω_0 is the initial angular velocity, t_s^0 is the time of braking with constant deceleration.

The opposite approach is presented in Type B. It is assumed, that the pressure varies with time (Chichinadze et al., 1979)

$$p(t) = p_0\left(1 - e^{-\frac{t}{t_m}}\right), \ 0 \le t \le t_s, \quad (6)$$

where: t_m is the growing time. The angular velocity corresponds to pressure (6) and is equal (Yevtushenko et al., 1999)

$$\omega(t) = \omega_0\left[1 - \frac{t}{t_s^0} + \frac{t_m}{t_s^0}\left(1 - e^{-\frac{t}{t_m}}\right)\right], \ 0 \le t \le t_s, \quad (7)$$

4. MATHEMATICAL MODEL

To evaluate the contact temperature conditions, both analytical and numerical techniques have been developed. The starting point for the analysis of the temperature field in the disc volume is the parabolic heat conduction equation in the cylindrical coordinate system (r, θ, z) which is centered in the axis of disc and z points to its thickness (Nowacki, 1962)

$$\frac{\partial^2 T}{\partial r^2} + \frac{1}{r}\frac{\partial T}{\partial r} + \frac{1}{r^2}\frac{\partial^2 T}{\partial \theta^2} + \frac{\partial^2 T}{\partial z^2} = \frac{1}{k_d}\frac{\partial T}{\partial t}, r_d \le r \le R_d, \quad (8)$$
$$0 \le \theta \le 2\pi, 0 < z < \delta_d, t > 0$$

where k_d is the thermal diffusivity of the disc, r_d and R_d are he internal and external radius of the disc. In an automotive disc brakes the Peclet numbers almost always are in order 10^5. Hence the distribution of heat flow will be uniform in circumferential direction, which means that neither temperature nor heat flow will vary in θ direction and thus the heat conduction equation reduces to

$$\frac{\partial^2 T}{\partial r^2} + \frac{1}{r}\frac{\partial T}{\partial r} + \frac{\partial^2 T}{\partial z^2} = \frac{1}{k_d}\frac{\partial T}{\partial t}, r_d \le r \le R_d, 0 < z < \delta_d, t > 0, \quad (9)$$

The boundary and initial conditions are given as follows:
Type A

$$K_d \frac{\partial T}{\partial z}\bigg|_{z=\delta_d} = \begin{cases} h[T_a - T(r,\delta_d,t)], \ r_d \le r \le r_p, \ t \ge 0, \\ q_d(r,\delta_d,t), \ r_p \le r \le R_p, \ 0 \le t \le t_s, \end{cases} \quad (10)$$

where T_a is the ambient temperature.

$$K_d \frac{\partial T}{\partial r}\bigg|_{r=R_d} = h[T_a - T(R_d,z,t)], \ 0 \le z \le \delta_d, \ t \ge 0, \quad (11)$$

$$K_d \frac{\partial T}{\partial r}\bigg|_{r=r_d} = -h[T_a - T(r_d,z,t)], \ 0 \le z \le \delta_d, \ t \ge 0, \quad (12)$$

$$\frac{\partial T}{\partial z}\bigg|_{z=0} = 0, \ r_d \le r \le R_d, \ t \ge 0, \quad (13)$$

$$T(r,z,0) = T_0, \ r_d \le r \le R_d, \ 0 \le z \le \delta_d, \quad (14)$$

Type B

$$K_d \frac{\partial T}{\partial z}\bigg|_{z=\delta_d} = \begin{cases} h[T_a - T(r,\delta_d,t)],\ r_d \le r \le r_p \wedge R_p \le r \le R_d, t \ge 0, \\ q_d(r,\delta_d,t), r_p \le r \le R_p,\ t \ge 0, \end{cases} \quad (15)$$

$$K_d \frac{\partial T}{\partial r}\bigg|_{r=R_d} = h[T_a - T(R_d,z,t)],\ 0 \le z \le \delta_d,\ t \ge 0, \quad (16)$$

$$\frac{\partial T}{\partial r}\bigg|_{r=r_d} = 0,\ 0 \le z \le \delta_d,\ t \ge 0, \quad (17)$$

$$\frac{\partial T}{\partial z}\bigg|_{z=0} = 0,\ r_d \le r \le R_d,\ t \ge 0, \quad (18)$$

$$T(r,z,0) = T_0,\ r_d \le r \le R_d,\ 0 \le z \le \delta_d, \quad (19)$$

The above cases are two-dimensional problem for transient analysis. The boundary and initial conditions are specified for subsequent types of disc.

5. FE FORMULATION

The object of this section is to develop approximate time-stepping procedures for axisymmetrical transient governing equations. For this to happen, the following boundary and initial conditions are considered

$$T = T_p \text{ on } \Gamma_T \quad (20)$$

$$q = -h(T - T_a) \text{ on } \Gamma_h \quad (21)$$

$$q = q_d \text{ on } \Gamma_q \quad (22)$$

$$T = T_0 \text{ on at time } t = 0 \quad (23)$$

where T_p is the prescribed temperature, Γ_T, Γ_h, Γ_q, are arbitrary boundaries on which temperature, convection and heat flux are prescribed.

In order to obtain matrix form of Eq. (9) the application of standard Galerkin's approach was conducted (Lewis et al., 2004). The temperature was approximated over space as follows

$$T(r,z,t) = \sum_{i=1}^{n} N_i(r,z) T_i(t) \quad (24)$$

where: N_i are shape functions, n is the number of nodes in an element, $T_i(t)$ are time dependent nodal temperatures.

The standard Galerkin's approach of Eq. (9) leads to the following equation

$$\int_\Omega K_d N_i \left[\frac{\partial^2 T}{\partial r^2} + \frac{1}{r}\frac{\partial T}{\partial r} + \frac{\partial^2 T}{\partial z^2} - \rho_d c_d \frac{\partial T}{\partial t} \right] d\Omega = 0 \quad (25)$$

Using integration by parts of Eq. (25) we obtain

$$-\int_\Omega K_d \left[\frac{\partial N_i}{\partial r}\frac{\partial T}{\partial r} + \frac{\partial N_i}{\partial z}\frac{\partial T}{\partial z} - \frac{N_i}{r}\frac{\partial T}{\partial r} + N_i \rho_d c_d \frac{\partial T}{\partial t} \right] d\Omega + \int_\Gamma K_d N_i \frac{\partial T}{\partial r} l d\Gamma + \int_\Gamma K_d N_i \frac{\partial T}{\partial z} n d\Gamma = 0 \quad (26)$$

Integral form of boundary conditions

$$\int_\Gamma K_d N_i \frac{\partial T}{\partial r} l d\Gamma + \int_\Gamma K_d N_i \frac{\partial T}{\partial z} n d\Gamma = -\int_{\Gamma_q} N_i q_d d\Gamma_q - \int_{\Gamma_h} N_i h(T - T_a) d\Gamma_h \quad (27)$$

Substituting Eq. (27) and spatial approximation Eq. (24) to Eq. (26) we obtain

$$-\int_\Omega K_d \left[\frac{\partial N_i}{\partial r}\frac{\partial N_j}{\partial r} + \frac{\partial N_i}{\partial z}\frac{\partial N_j}{\partial z} - \frac{N_i}{r}\frac{\partial N_j}{\partial r} \right] T_j d\Omega - \int_\Omega \rho_d c_d N_i \frac{\partial N_j}{\partial t} T_j d\Omega - \int_{\Gamma_q} N_i q_d d\Gamma_q - \int_{\Gamma_h} N_i h(T - T_a) d\Gamma_h = 0 \quad (28)$$

where i and j represent the nodes.
Equation (28) can be written in matrix form

$$[C]\left\{\frac{\partial T}{\partial t}\right\} + [K][T] = \{R\} \quad (29)$$

where $[C]$ is the heat capacity matrix, $[K]$ is the heat conductivity matrix, and $\{R\}$ is the thermal force matrix.
or

$$[C_{ij}]\left\{\frac{\partial T_j}{\partial t}\right\} + [K_{ij}][T_j] = \{R_i\} \quad (30)$$

where

$$[C_{ij}] = \int_\Omega \rho_d c_d N_i N_j d\Omega \quad (31)$$

$$[K_{ij}] = \int_\Omega K_d \left(\frac{\partial N_i}{\partial r}\frac{\partial N_j}{\partial r}\{T_j\} + \frac{\partial N_i}{\partial z}\frac{\partial N_j}{\partial z}\{T_j\} - \frac{N_i}{r}\frac{\partial N_j}{\partial r}\{T_j\} \right) d\Omega + \int_\Gamma h N_i N_j d\Gamma \quad (32)$$

$$[R_i] = -\int_{\Gamma_q} q_d N_i d\Gamma_q + \int_{\Gamma_h} N_i h T_a d\Gamma_h \quad (33)$$

or in matrix form

$$[C] = \int_\Omega \rho_d c_d [N]^T [N] d\Omega \quad (34)$$

$$[K] = \int_\Omega [B]^T [D][B] d\Omega + \int_\Gamma h [N]^T [N] d\Gamma \quad (35)$$

$$\{R\} = -\int_{\Gamma_q} q_d [N]^T d\Gamma_q + \int_{\Gamma_h} h T_a [N]^T d\Gamma_h \quad (36)$$

In order to solve the ordinary differential equation (29) the direct integration method was used. Based on the assumption that temperature $\{T\}_t$ and $\{T\}_{t+\Delta t}$ at time t and $t+\Delta t$ respectively, the following relation is specified

$$\{T\}_{t+\Delta t} = \{T\}_t + \left[(1-\beta)\left\{\frac{\partial T}{\partial t}\right\}_t + \beta \left\{\frac{\partial T}{\partial t}\right\}_{t+\Delta t} \right] \Delta t \quad (37)$$

Substituting Eq. 37 to Eq. 29 we obtain the following implicit algebraic equation

$$\left([C]+\beta\Delta t[K]\right)\{T\}_{t+\Delta t}=\left([C]-(1-\beta)[K]\Delta t\right)\{T\}_t + (1-\beta)\Delta t\{R\}_t+\beta\Delta t\{R\}_{t+\Delta t} \tag{38}$$

where β is the factor which ranges from 0.5 to 1 and is given to determine an integration accuracy and stable scheme.

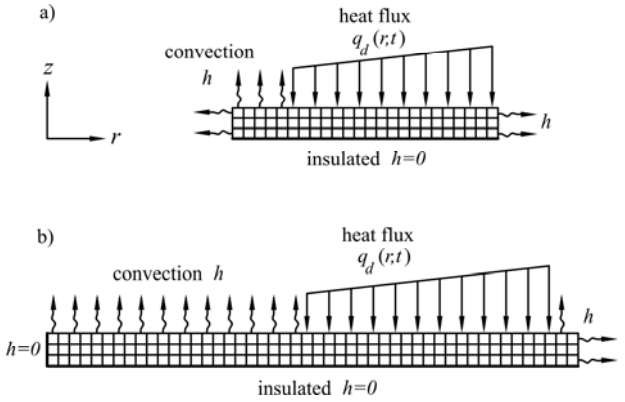

Fig. 3. FE models with boundary conditions for the transient analysis a) Type A, b) Type B

The finite element formulation of disc brakes with boundary conditions is shown in Fig. 3. Two FE models described below were analyzed using the MD Patran/MD Nastran software package (Reference Manual MD Nastran, 2008; Reference Manual MD Patran, 2008). In the thermal analysis of disc brakes an appropriate finite elements division is indispensable. In this paper eight-node quadratic elements were used for finite element analysis. Type A consists of 235 elements and 810 nodes and Type B 570 elements and 1913 nodes. High order of elements ensure appropriate numerical accuracy.

To avoid inaccurate or unstable results, a proper initial time step associated with spatial mesh size is essential (Reference Manual MD Nastran, 2008).

$$\Delta t=\Delta x^2\frac{\rho_d c_d}{10K_d} \tag{39}$$

where Δt is the time step, Δx is the mesh size (smallest element dimension). In this paper fixed Δt =0.005s time step was used.

6. RESULTS AND DISCUSSION

In this paper temperature distributions in disc brake model without pad have been investigated. It is connected with its sophisticated behaviour and importance of operation. Disc material is subjected to high temperatures action which may cause non-uniform pressure distribution, thermal distortions, low frequency vibrations. Both convection and conduction have been analyzed. Particularly conduction was considered to be the most important mode of heat transfer.

In order to validate proposed transient numerical analysis two different types of the FE model were investigated (Talati and Jalalifar, 2009; Gao and Lin, 2002). A transient solution for Type A was performed for operation conditions of constant contact pressure p_0=3.17MPa and initial angular velocity ω_0=88.46s^{-1} during 3.96s of braking process (Fig. 4a). Evolution of the pressure p and angular velocity of the disc ω for Type B is shown in Fig. 4b. Material properties and operation conditions adopted in the analysis for both types of disc numerical model are given in Tab. 1 and Tab. 2 respectively.

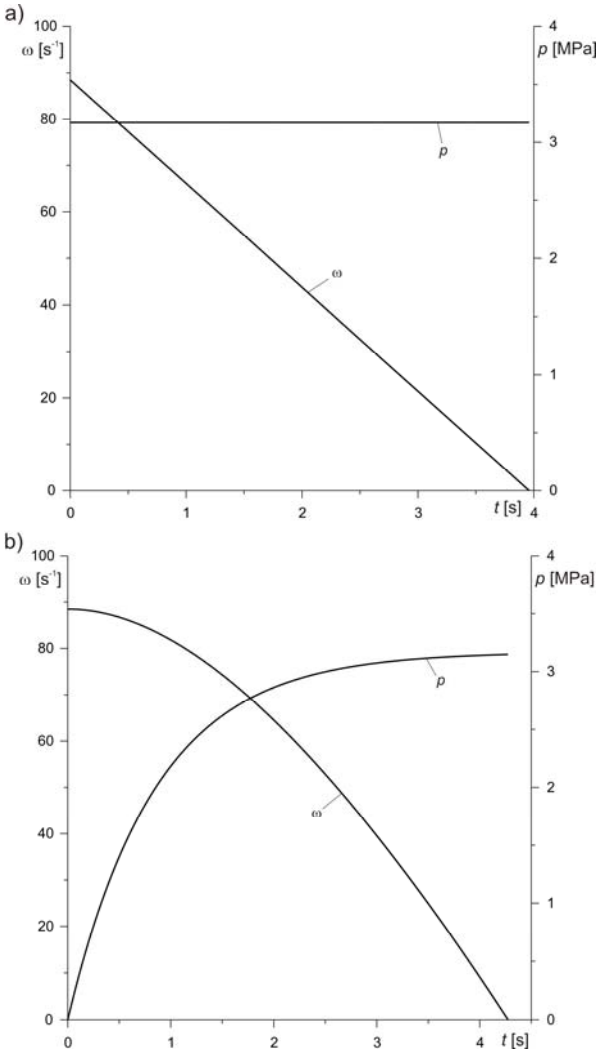

Fig. 4. Evolution of the pressure p and angular velocity ω during braking: a) Type A, b) Type B

Fig. 5a shows disc surface temperature distribution for transient numerical computation (Type A) at different radial distances. As it can be seen values of temperature increase with radial distances. The highest temperature of brake exert occurs at 113.5mm of radial position and t=3.025s of time. Temperature distribution corresponds intermediately to the intensity of heat flux, which rises with time until the value of velocity and pressure product attains highest, critical value. Hence temperature indirectly increases with time and decreases when the intensity of heat flux q_d descents. The slope $\partial T/\partial t$ of plots r=75.5mm, r=80mm, r=90mm, r=100mm, r=113.5mm decreases with time. It agree well with Talati and Jalalifar's paper (2009) with distinction to values of temperatures. In this paper the

highest temperature of disc area, which occurs during emergency braking achieves 227.90^{0}C. Meanwhile maximum temperature obtained in Talati's model of disc brake is higher and equals approximately 300^{0}C.

Fig. 5b shows disc temperature surface variations along radial direction obtained in numerical computation for Type B. In opposite to constant pressure at the disc/pad interface, in this case pressure differs with time (Fig. 4b.). Also angular velocity has been assumed as a nonlinear. As it can be seen temperature at inner disc surface (r=52 mm) has a constant value 20^{0}C. It corresponds to boundary conditions, where surface was insulated. Maximum temperature rise up to 280.9^{0}C at 113mm of radial position and 3.49s of time.

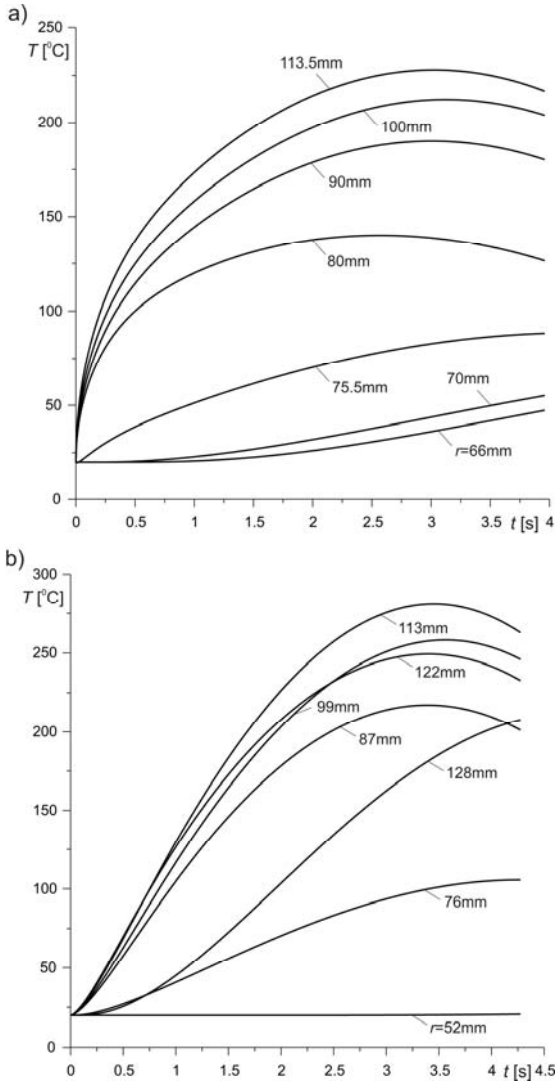

Fig. 5. Evolution of the disc temperature on the friction surface for different values of the radial position:
a) Type A, b) Type B

In Fig. 6a disc temperature in Type A at r=113.5mm and at different axial positions is illustrated. Symmetry in axial direction has been assumed. Hence plots from z=0mm to maximum thickness of the disc are shown. At the initial period of disc brake engagement maximum temperature distribution appears at the disc/pad interface (z=5.5mm). There is a tendency to convergence of temperature at different axial positions at the end of braking process. It is connected with alignment of temperatures in disc brake in subsequent stage of the process when the intensity of heat flux descents. Temperature of plots z=4.4mm, z=5.5mm rises with time to 3.47s and 3.025s respectively.

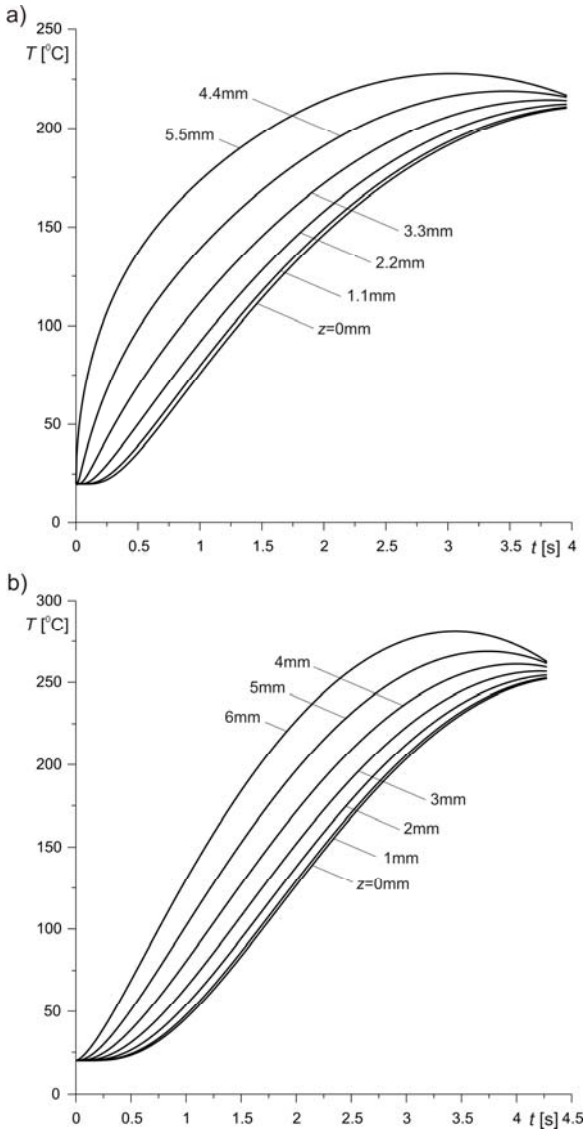

Fig. 6. Evolution of the disc temperature at different axial distances and at radial position:
a) r=113.5mm (Type A) b) r=113mm (Type B)

In Fig. 6b temperature distribution at r=113mm in different axial distances is shown. As it can be seen temperature of plots z=4mm, z=5mm, z=6mm increases with time to 4s, 3.74s and 3.44s respectively and then decreases while temperature of plots z=0mm, z=1mm, z=2mm, z=3mm constantly grows.

Tab. 1. Material properties used in finite element analysis

Thermo-physical properties	Type A [13]		Type B [3]	
	Disc	Pad	Disc	Pad
thermal conductivity, K_d [W/mK]	43	12	48.46	1.212
heat capacity, c_d [J/kgK]	445	900	419	1465
density, ρ_d [kg/m^3]	7850	2500	7228	2595

Tab. 2. Operation conditions for the transient numerical analysis

Items	Type A [13]		Type B [3]	
	Disc	Pad	Disc	Pad
inner radius, $r_{d,p}$[mm]	66	76.5	32.5	77
outer radius, $R_{d,p}$ [mm]	113.5		128	125
cover angle of pad, ϕ_0		64.5		64.5
disc thickness δ_d [mm]	5.5		6	
initial velocity ω_0 [s^{-1}]	88.46		88.46	
time of braking, t_s [s]	3.96		4.274	
pressure p_0 [MPa]	3.17		3.17	
coefficient of friction f	0.5		0.5	
heat transfer coefficient h [W/m^2K]	60		100	
initial temperature T_0 [^{0}C]	20		20	
ambient temperature T_a [^{0}C]	20		20	
time step Δt [s]	0.005		0.005	

7. CONCLUSION

In this paper transient thermal analysis of disc brakes in single brake application was performed. To obtain the numerical simulation parabolic heat conduction equation for two-dimensional model was used. The results show that both evolution of rotating speed of disc and contact pressure with specific material properties intensely effect disc brake temperature fields in the domain of time. Proposed transient FE modeling technique of two types of braking engagement model agrees well with papers Talati and Jalalifar (2009), Gao and Lin (2002). An instant pressure action of disc/pad interface (Type A) pronouncedly implies temperature growth at initial period of brake exert. More slightly temperature rise in Type B has been noticed. The highest temperature occurs approximately at 3s, 3.5s into the braking process for the period of 3.96s, 4.274s time in Type A and Type B respectively. The present paper is a preliminary of subsequent investigation with nonlinear variations of applied thermal characteristics.

REFERENCES

1. **Blok H.** (1940), Fundamental Mechanical Aspects in Boundary Lubrication, *SAE Trans*., Vol. 46, 54-68.
2. **Chichinadze A. V., Braun E. D., Ginsburg A. G. et al.** (1979), *Calculation, test and selection of frictional couples*, Science, Moscow *(in Russian).*
3. **Gao C. H., Lin X. Z.** (2002), Transient temperature field analysis of a brake in a non-axisymmetric three-dimensional model, *J. Mater. Proc. Technol.*, Vol. 129, No 1, 513–517.
4. **Grieve D. G., Barton D. C., Crolla D. A., Buckingham J. T.** (1998), Design of a lightweight automotive brake disc using finite element and Taguchi techniques, *Proc. Instn. Mech. Engrs.,* Vol. 212, No 4, 245-254.
5. **Lewis R. W., Nithiarasu P., Seetharamu K. N.** (2004), *Fundamentals of the finite element method for Heat and Fluid Flow*, John Wiley & Sons.
6. **Ling F. F.** (1973), *Surface mechanics*, John Wiley & Sons, New York.
7. **Nowacki W.** (1962), *Thermoelasticity*, Pergamon Press, Oxford.
8. **Ramachandra Rao V. T. V. S., Ramasubramanian H. and Seetharamu K. N.** (1989), Analysis of temperature field in brake disc for fade assessment, *Wärme- und Stoffübertragung*, Vol. 24, No 1, 9-17.
9. **Ścieszka S., Żołnierz M.** (2007), Wpływ cech konstrukcyjnych hamulca tarczowego maszyny wyciągowej na jego niestabilność termosprężystą. Część I. Budowa modelu MES i jego weryfikacja, *Zagadnienia Eksploatacji Maszyn*, Vol. 42, No 3, 111-124.
10. **Ścieszka S., Żołnierz M.** (2007), Wpływ cech konstrukcyjnych hamulca tarczowego maszyny wyciągowej na jego niestabilność termosprężystą. Część II. Badania symulacyjne, *Zagadnienia Eksploatacji Maszyn*, Vol. 42, No 4, 183-193.
11. **Taguchi G.** (1993), *Taguchi on Robust Technology Development*, ASME Press, New York.
12. **Talati F., Jalalifar S.** (2008), Investigation of heat transfer phenomena in a ventilated disk brake rotor with straight radial rounded vanes, *Journal of Applied Sciences*, Vol. 8, No 20, 3583-3592.
13. **Talati F., Jalalifar S.** (2009), Analysis of heat conduction in a disk brake system, *Heat Mass Transfer*, Vol. 45, No 8, 1047-1059.
14. **Yevtushenko A. A., Ivanyk E. G., Yevtushenko O. O.** (1999), Exact formulae for determination of the mean temperature and wear during braking. *Heat and Mass Transfer*, Vol. 35, No 2, 163–169.
15. **MSC.Software** (2008), *Reference Manual MD Nastran, Version r2.1.*
16. **MSC.Software** (2008), *Reference Manual MD Patran, Version r2.1.*